Identification and Characterization of the *MDR1* Promoter-Enhancing Factor 1 (MEF1) in the Multidrug Resistant HL60/VCR Human Acute Myeloid Leukemia Cell Line†

Besim Ogretmen‡ and Ahmad R. Safa*

Medical University of South Carolina, Hollings Cancer Center, 86 Jonathan Lucas Street, P.O. Box 250955, Charleston, South Carolina 29425

Received August 19, 1999; Revised Manuscript Received October 26, 1999

ABSTRACT: In this report, the molecular mechanisms involved in the overexpression of *MDR1* mRNA in the multidrug resistant variant of the HL60 human acute myeloid leukemia cell line, HL60/VCR, were investigated. RT-PCR and nuclear run-on assays revealed that the expression of *MDR1* mRNA is regulated by increased transcriptional initiation in HL60/VCR cells. Transient transfections with a 241 bp *MDR1* promoter (spanning the −198 to +43 region) DNA fragment/pGL3-basic plasmid construct resulted in about 6-fold increased luciferase activity in HL60/VCR but not in HL60 cells. Moreover, ds CAAT-oligomer from the *MDR1* promoter cloned upstream of the SV-40 promoter in the pGL3-promoter plasmid caused about a 7-fold increase in luciferase activity compared with plasmid constructs containing CAAT-deleted, GC-box, and nonspecific oligomers in HL60/VCR transfectants. These results were confirmed by transfecting HL60/VCR cells with the pGL3-basic plasmid containing a 237 bp mutated *MDR1* proximal promoter lacking the CAAT sequence in which no change in luciferase activity was observed. However, a 5−6-fold increase in luciferase activity was measured in these cells when transfected with the wt *MDR1* promoter DNA/pGL3-basic plasmid constructs. These results show that the CAAT-region is involved in upregulating the *MDR1* promoter in HL60/VCR cells. A nuclear factor binding to the CAAT-region of the *MDR1* promoter specifically was detected in electrophoretic mobility shift assays (EMSAs) in HL60/VCR but not in HL60 extracts. Two MDR1 promoter-associated polypeptides with molecular masses of about 130 and 162 kDa were identified in HL60/VCR cells by electroelution, specific DNA-affinity chromatography, and silver staining. Interestingly, cross-linking and Southwestern analysis indicate that only the 130 kDa protein, which we refer to as *MDR1*-promoter enhancing factor 1 (MEF1), has a strong DNA-binding ability, interacting with the 5′-GTCAATCC-3′ element of the *MDR1* promoter, as determined by DNase I protection assay. These data reveal that MEF1 upregulates the MDR1 promoter activity.

The development of resistance to a wide variety of chemotherapeutic agents presents a major clinical obstacle in the treatment of human cancers. One of the mechanisms involved in the development of multidrug resistance (MDR)[1] in human cancer cells is the overexpression of P-glycoprotein (P-gp), a product of the *MDR1* gene. P-gp is an ATP-dependent transmembrane efflux pump with high affinity for a number of structurally unrelated compounds (*1*−*3*). While the expression of P-gp has been demonstrated in many types of solid tumors (*4*-*6*), its correlation to the clinical outcome of chemotherapy in these tumors has not been well established. The best correlation between P-gp expression and treatment failure as a result of resistance to chemotherapy has been demonstrated in hematological malignancies (*7*). These include acute myelogenous and lymphocytic leukemias (AML and ALL), multiple myeloma, and non-Hodgkin's lymphoma (*7*). Moreover, clinical studies have shown that the P-gp expression alone in AML is a negative prognostic indicator (*8*−*10*), particularly in the elderly (*11*). It has been also shown that the overexpression of P-gp in hematological malignancies occurs more frequently at relapse than upon initial presentation (*12*).

There is sufficient evidence that the P-gp overexpression is mainly regulated at the transcriptional level by increased *MDR1* promoter activity (*4*, *13*). The *MDR1* promoter region contains recognition sites for a variety of transcription factors such as SP1, NF-Y, and YB-1, which are involved upregulating *MDR1* promoter activity in some human cancer cells (*13*-*15*). Moreover, it has been reported that the cyclic AMP-dependent protein kinase (cAMP−PK) signaling pathway

† This work was supported by research grants from the National Cancer Institute (CA 56078) and research supports from Hollings Cancer Center to ARS.

* To whom correspondence should be addressed at Indiana University Cancer Research Institute, 1044 West Walnut R4-119, Indianapolis, IN 46202. Phone: (317) 278-4952. Fax: (317) 274-8046.

‡ Present Address: Medical University of South Carolina, Department of Biochemistry and Molecular Biology, Strom Thurmond Building, 114 Doughty Street, Room 605, P.O. Box 250777, Charleston, SC 29425.

[1] Abbreviations: EMSA, electrophoretic mobility shift assay; PAGE, polyacrylamide gel electrophoresis; P-gp, P-glycoprotein; MDR, multidrug resistance; MRP, multidrug resistance-associated protein; AML, acute myeloid leukemia; TCA, tricholoroacetic acid; β-gal; β-galactosidase; ONPG, *o*-nitrophenyl β-D-galactopyranoside; EtBr, ethidium bromide; FCS, fetal calf serum, VCR, vincristine; VBL, vinblastine; DOX, doxorubicin; MEF1, MDR1 enhancing factor 1; HAT, histone acetyl transferase; HDAC, histone diacetylase; ANT2, adenine nucleotide translocator isoform 2.

10.1021/bi991943f CCC: $19.00
Published on Web 12/11/1999

might be linked to upregulation of the *MDR1* promoter by activating SP1 (*16*). In addition, the possible roles of the histone-modifying enzymes histone acetyl transferase (HAT) and histone deacetylase (HDAC) in regulating *MDR1* promoter activity mediated by NF-Y have been reported in the SW620 human colon carcinoma cell line (*17*). It was also reported that the nuclear factor NF-R1 is involved in the negative regulation of *MDR1* gene transcription in DOX resistant K562 cells (*18*). Recently, we have shown that cross-coupling of the NF-κB/p65 and c-Fos transcription factors exerts a negative regulatory function on *MDR1* promoter activity by interacting with the CAAT region of the promoter in sensitive MCF-7 human breast cancer cells, but not in its drug-resistant variant MCF-7/Adr cells expressing high levels of *MDR1* mRNA (*19*). Taken together, these results provide evidence that the *MDR1* promoter is under complex regulatory mechanisms and that there might be tissue-specific variations in its regulation. The data presented in this study show that P-gp is highly expressed in the multidrug resistant HL60/VCR human AML cell line compared to its sensitive parental HL60 cells. The molecular mechanisms which are involved in upregulating *MDR1* gene expression in these cells have not been explored previously. Therefore, in this study, we attempted to identify the nuclear factors involved in the control of *MDR1* promoter activity in HL60 and HL60/VCR cells. We report here the identification, characterization, and purification of a protein complex which is involved in upregulating *MDR1* promoter activity by interacting with the 5′-GTCAATCC-3′-region of the promoter in HL60/VCR cells.

EXPERIMENTAL PROCEDURES

Cell Lines and Culture Conditions. The HL60 human AML cell line, its MDR1-mediated multidrug resistant derivative HL60/Vinc, and its MRP-mediated variant HL60/Adr cells were obtained from Dr. Melvin S. Center (Division of Biology, Kansas State University, Manhattan, KS). The derivative of HL60/Vinc cells expressing high levels of P-gp, referred to as HL60/VCR, was isolated by stepwise selection of HL60/Vinc cells exposed to increasing concentration of vincristine in our laboratory (Safa, unpublished data). Cells were maintained in RPMI-1640 medium with 10% fetal calf serum (FCS) and 100 ng/mL each of penicillin and streptomycin (Life Technologies, Grand Island, NY) at 37 °C in 5% CO_2. HL60/VCR cells were grown in the presence of 1 μg/mL vincristine which was removed from the media 1 week before each assay. Vincristine and vinblastine were obtained from Eli Lilly and Co. (Indianapolis, IN) and doxorubicin was purchased from Sigma Chemical Co. (St. Louis, MO).

Cell Survival (MTT) Assay. Cells (1×10^4 cells/well) were plated in 100 μL of the growth medium in the absence or presence of increasing concentrations of chemotherapeutic drugs into 96-well plates at 37 °C in 5% CO_2 for 72 h. The cells were then incubated with 25 μL of 3-[4,5-dimethylthiazol-2-yl]-2,5-diphenyltetrazolium bromide (MTT) (5 mg/mL) at 37 °C for 4 h. After lysing, plates were read in a microplate reader (Dynatech Laboratories; Chantilly, VA) at 570 nm, and the concentration of drug that inhibited cell survival by 50% (IC_{50}) was determined from cell survival plots (*20*).

Western Blot Analysis. Protein levels of P-gp in cells were measured by Western blot analysis as we described elsewhere (*21*). In short, total proteins (50 μg/lane) were separated by 5−15% SDS−PAGE containing 6.5 M urea, blotted onto an Immobilon membrane, and then P-gp levels were detected using 1 μg/mL of mouse monoclonal C219 antibody that recognizes P-gp and peroxidase-conjugated secondary anti-mouse antibody (1:2500). The proteins were visualized using the ECL protein detection kit (Amersham, Arlington Heights, IL) as described by manufacturer. The membranes were then exposed to Kodak X-Omat film for various times. Equal loading was confirmed by Coomassie blue staining of SDS−PAGE strips cut from gels containing 50 μg of protein/lane of each sample prior to blotting. The protein levels were quantitated by densitometry of the autoradiograms.

Isolation of Total RNA and RT-PCR. MDR1 mRNA levels were analyzed by RT-PCR as previously described (*19*). In short, total RNA from HL60 and HL60/VCR cells was isolated using a modified SDS-phenol technique (*22*) and then 1 μg of total RNA was used in reverse transcription reactions with AMV-reverse transcriptase and random primers (Promega, Madison, WI) as described by manufacturer. The resulting total cDNA was then used in PCR to measure the *MDR1* mRNA levels. The intactness of total RNA was confirmed by tight bands of 28S and 18S rRNA separated on denaturing agarose gels and visualized by ethidium bromide (EtBr) staining (*23*). The primers and amplification conditions of PCR were as follows:

MDR1 (forward), 5′ CCCATCATTGCAATAGCAGG (2596−2615)

MDR1 (reverse), 5′ GTTCAAACTTCTGCTCCTGA (2733−2752)

β-actin (forward), 5′ CAGAGCAAGAGAGGCATCCT (216−235)

β-actin (reverse), 5′ TTGAAGGTCTCAAACATGAT (405−424)

The reactions were performed at 94 °C for denaturation, 60 °C for annealing, and 72 °C for amplification for 30 cycles. The β-actin mRNA levels were used as internal controls in RT-PCR. The amplified fragments were separated on 2% agarose gels and visualized by EtBr staining.

Nuclear Run-On Transcription Assay. Nuclear run-on analysis was performed as previously described (*24*). Briefly, nuclei from HL60 and HL60/VCR cells were isolated and stored in 100 μL of freezing buffer (50 mM Tris-HCl, pH 8.3, 40% glycerol, 5 mM $MgCl_2$ and 0.1 mM EDTA). For analysis, nuclei were thawed and incubated with 100 μL of reaction buffer containing 10 mM Tris-HCl, pH 8.0, 5 mM $MgCl_2$, 300 mM KCl, 0.5 mM each of ATP, CTP, GTP, and 150−200 μCi of [α-^{32}P]UTP at 30 °C for 30 min. Reactions were stopped by DNase I (100 units) treatment at 30 °C for 20 min. Following deproteinization by proteinase K (25 μg/mL) at 42 °C for 30 min, the labeled transcripts were extracted by phenol/chloroform (49:1) and then precipitated using ethanol and sodium acetate. Equal counts of TCA-precipitated labeled transcripts were used for hybridizations of slot blots containing 0.4 μg of full-length 4.2 kb

human *MDR1* and 1.8 kb human β-actin (CloneTech, Palo Alto, CA) cDNA fragments. Hybridizations were performed at 45 °C for 72−96 h and then the filters were washed at 57 °C with 2× SSC-1% SDS and 0.1× SSC-1% SDS for 1−2 h as we previously described (*24*). Bands were visualized by autoradiography at −80 °C for 7−10 days.

Preparation of MDR1 Promoter Fragment by PCR. The 241 bp *MDR1* promoter fragment spanning −198 to +43 sites was produced by PCR using HL60/VCR genomic DNA as a template with the following primers as we described previously (*19*):

MDR1 promoter
(forward) 5′ CTAGAGAGGTGCAACGGA
(−198 to −181)

MDR1 promoter
(reverse) 5′ GCGGCCTCTGCTTCTTTGA
(+25 to +43)

Amplification conditions were as described above except that 5% deionized formamide was added to the reaction and the annealing temperature was 55 °C. The 241 bp PCR product was then separated on 2% agarose gels and purified using the Qiaex II gel extraction kit (Qiagen, Valencia, CA) as described by the manufacturer prior to end-labeling reactions.

Plasmid Constructions. The 241 bp *MDR1* promoter fragment (−198 to +43) was amplified by PCR using primers 1 and 4, containing *Nhe*I and *Bgl*II sites (underlined sequences), respectively, as described (*19*). The 237 bp mutant *MDR1* promoter fragment lacking the CAAT motif (−116 to −113) was generated by two independent PCRs with primers 1−2 and 3−4, respectively, using the wild-type (wt) 241 bp *MDR1* promoter DNA fragment generated by PCR as a template. The overlapping primers 2 and 3 contain a deletion at the −116 to −113 sites (CAAT) of the *MDR1* promoter. The PCR products above were gel purified separately and then used as templates in a third PCR with primers 1 and 4 to generate the mutated 237 bp *MDR1* promoter fragment lacking the CAAT motif. The CAAT-deleted 237 bp *MDR1* promoter fragment was purified from 2% agarose gels and then cloned into pGL3-basic as described. The DNA sequences of the wt (241 bp) or mutated (237 bp) *MDR1* promoter fragments were confirmed by direct sequencing. The sequences of the primers above were as follows:

Primer 1: 5′ GCGCTAGCCTAGAGAGGTGCAACG
(−198 to −182)

Primer 2:
5′ CCCGGCCCGGACTGAATGCTGATTCCTC
(−103 to −112 and −117 to −134)

Primer 3:
5′ AGGAATCAGCCGGGCCGGGAGCAGTC
(−133 to −124 and −112 to −96)

Primer 4: 5′ GCAGATCTGCGGCCTCTGCTTCTT
(+28 to +43)

The ds-oligonucleotides containing CAAT-like motif, GC-box-like motif, CAAT-deleted motif, and nonspecific motif were synthesized and annealed by Midland Certified Reagent Co. (Midland, TX). These oligonucleotides are designed to contain 5′ *Nhe*I and 3′ *Bgl*II compatible (sticky) ends (underlined sequences) to clone into the pGL3-promoter vector (Promega) containing the SV-40 promoter downstream of the cloning sites, as described above. The DNA sequences of the oligonucleotides were as follows:

CAAT-like motif: P-CTAGCAATCAGCATTCAGTC-
AATCCGGGCCAGTTAGTCGTAAGTCAGTTAG-
GCCCGGTCTAG-P

CAAT-deleted motif: P-CTAGCAATCAGCATTCA-
GTCCGGGCCAGTTAGTCGTAAGTCAGGCCC-
GGTCTAG-P

GC-box like motif: P-CTAGCGGAACAGCGCCGG-
GGCGTGGGCTGAAGCCTTGTCGCGGCCCC-
GCACCCGACTTCTAG-P

Nonspecific motif: P-CTAGCGGAAGCCTGAGCT-
CATTCGAGTAGCAGCCTTCGGACTCGAG-
TAAGCTCATCGTCTAG-P

The cloning of these oligonucleotides into the pGL3-promoter vector was confirmed by restriction enzyme digestions and direct sequencing. All of the resulting plasmids were amplified in *Escherichia coli* JM109 and then isolated using the Qiagen plasmid isolation kit before transfection as described by manufacturer.

Transient Transfections and Luciferase and β-Galactosidase Assays. Cells [(2−5) × 10^5 cells/well] were seeded into 6-well plates and grown in 5 mL of the growth medium with 10% FCS for 18 h before transfections. The cells were then cotransfected with 2.5−3 μg/well plasmid constructs and pSV-β-galactosidase control plasmid (Promega) by cationic liposome-mediated transfection method using the DOTAP transfection kit (Boehringer-Mannheim) for 6−8 h as described by the manufacturer. After the transient transfectants were recovered in fresh media for 18 h, luciferase and β-galactosidase (β-gal) activities were measured using Promega's luciferase and β-gal enzyme assay systems as described by manufacturer. In short, cells were lysed in 400 μL of the reporter lysis buffer containing 25 mM Tris-phosphate, pH 7.8, 2 mM DTT, 2 mM diaminocyclohexane-*N*,*N*,*N*′,*N*′-tetraacetic acid, 10% glycerol, and 1% Triton X-100 at room temperature for 15 min. The luciferase reaction was then initiated by autoinjection of 100 μL of luciferase assay reagent containing 20 mM tricine, 1.07 mM $(MgCO_3)_4$ $Mg(OH)_2 \cdot 5H_2O$, 2.67 mM $MgSO_4$, 0.1 mM EDTA, 33.3 mM DTT, 270 μM coenzyme A, 470 μM luciferase, and 530 μM ATP to 20 μL of lysates using a luminometer (Turner Designs, Sunnyvale, CA). The light intensity of the luciferase reactions measured in the lysates of the transient transfectants were normalized to their β-gal activity, used as an internal control. The β-gal activity of the lysates was determined as follows: 120 μL of lysates in reporter lysis buffer was incubated with 150 μL of assay buffer containing 200 mM sodium phosphate, pH 7.3, 2 mM $MgCl_2$, 100 mM β-mercaptoethanol, and 1.33 mg/mL *o*-nitrophenyl β-D-galactopyranoside (ONPG) at 37 °C for 30 min. The reaction was stopped by the addition of 1 M sodium carbonate and then read using a spectrophotometer

at 420 nm. All of the transfections and assays were performed in triplicate.

Preparation of Nuclear Extracts. The nuclear extracts from HL60 and HL60/VCR cells were prepared as previously described (*19*). In summary, cells (about 10^9) grown in large flasks were scraped, washed with phosphate buffered-saline (PBS), pH 7.1, then lysed in buffer A containing 0.01 M Hepes, pH 7.5, 0.02 M $MgCl_2$, 0.015 M KCl, 0.1 mM EDTA, 0.001 M DTT, and 0.001 M PMSF. The nuclear pellet was then homogenized on ice by 10−20 strokes of an S-pestal and then spun at 13000*g* for 10 min. The nuclear proteins were cleared by adding 80 μL of 0.3 M ammonium sulfate for 30 min on ice. Following centrifugation at 50000*g* at 4 °C for 60 min, the clear nuclear protein suspension was reprecipitated with 0.2 g/mL ammonium sulfate. The pellets were collected by centrifugation at 50000*g* for 15 min and then resuspended in 500 μL of buffer C (0.05 M Hepes, pH 7.5, 0.03 M KCl, 0.1 mM EDTA, 0.001 M DTT, 0.001 M PMSF, and 10% glycerol). After the samples were dialyzed against buffer C (500× volume) at 4 °C for 18−24 h, they were cleared by microcentrifugation at 13000*g* for 10 min and stored at −80 °C. The concentration of nuclear protein was determined by the Bradford assay using the Bio-Rad (Richmond, CA) protein detection kit as described by manufacturer.

Electrophoretic Mobility Shift Assay (EMSA). Nuclear extracts (8−10 μg of protein) were preincubated in 15 μL of binding buffer (0.04 M Hepes, pH 7.5, 0.04 M KCl, 8% glycerol, 0.64 M PMSF, 0.8 mM DTT, and 0.1 mM EDTA) containing 1.5 μg of poly(dI·dC) (Pharmacia, Piscataway, NJ) with or without oligonucleotides used as competitors at 30 or 25 °C for 15 min. Then, 3−5 ng of 5′-end labeled DNA probes (60 000 cpm) were added to the reaction and incubated at 25 °C for 15 min. End labeling of DNA fragments with γ-[^{32}P]ATP (Amersham, Arlington Heights, IL) was performed using T4 DNA kinase (Promega), and the specific activity of the probes was determined by scintillation counting after TCA precipitation as described by manufacturer. Competitor double-stranded oligonucleotides were used at 10−100-fold molar excess. The 5′-end (forward) DNA sequences of ds-oligomers used in the gel shift assays were as follows:

CAAT-like motif:
ATCAGCATTCAGTCAATCCGGGCC

CAAT-deleted motif: ATCAGCATTCAGTCCGGGCC

GC-box-like motif:
GGAACAGCGCCGGGGCGTGGGCTGA

Nonspecific motif:
GAAGCCTGAGCTCATTCGAGTAGC

NF-κB motif: AGTTGAGGGGACTTTCCCAGGC

SP1 motif: ATTCGATCGGGGCGGGGCGAGC

AP1 motif: CGCTTGATGAGTCAGCCGGAA

C/EBP motif: TGCAGATTGCGCAATCTGCA

YY1 motif:
CGCTCCGCGGCCATCTTGGCGGCTGGT

The reaction mixtures were separated on 5% native polyacrylamide gels and autoradiography was performed by exposing dried gels to Kodak X-Omat films. The ds-oligonucleotides containing CAAT-like, CAAT-deleted, GC-box, and nonspecific motifs were synthesized and annealed by Midland Certified Reagent Co. The ds-oligomers containing NF-κB, SP1, and AP1 motifs were purchased from Promega. The ds-oligomers containing C/EBP and YY1 motifs were purchased from Santa Cruz Biotechnology (Santa Cruz, CA).

UV Cross-Linking of the DNA−Protein Complexes. The 5′-end labeled CAAT oligonucleotide probe (about 1.2×10^5 cpm) was incubated with 15 μg of nuclear extracts under the exact conditions described above in the EMSA. Samples were then placed 5 cm from a UV transilluminator and exposed to UV light (302 nm) for 15, 30, or 60 min on ice. Cross-linked complexes were then separated by 5−15% SDS−PAGE, the gels were fluorographed, and dried, and the signals were detected by autoradiography. DNase I treatment of the UV cross-linked probes was omitted due to the use of the 5′-end labeled oligomers in this assay.

Southwestern Blotting. Southwestern blot analysis was performed as described previously (*18*). The nuclear extracts were separated by 5−15% SDS−PAGE with 6.5 M urea and transferred to Immobilon membrane as described above. The membranes were blocked in blocking buffer containing 0.04 M Hepes, pH 7.5, 0.04 M NaCl, 1 mM EDTA, 1 mM DTT, and 5% dry milk for 1 h at 25 °C. The blots were then hybridized in the same buffer with the ^{32}P end-labeled CAAT oligomer (2×10^6 cpm/mL) and 10 μg/mL poly (dI·dC) for 1 h at 25 °C. The membranes were washed three times for 20 min in the same buffer without dry milk and the bands were visualized by autoradiography.

Purification of CAAT-Binding Protein by Electroelution. The nuclear factor which interacts with the CAAT-region of the *MDR1* promoter in HL60/VCR cells was purified from polyacrylamide gels following EMSAs by electroelution as described (*25*). In summary, after EMSAs were performed using CAAT-oligomer as a probe, protein−DNA complexes were separated on 5% native polyacrylamide gels as described above. Then, gel pieces containing the CAAT-binding nuclear protein were excised (the position of the shifted band in the polyacrylamide gel was determined by autoradiography) and protein−DNA complexes were eluted using Electroeluter model 422 (Bio-Rad) in electrode buffer containing 25 mM Tris-base, 192 mM glycine, and 1% SDS as described by manufacturer. The proteins were then separated and analyzed by 5−15% SDS−PAGE followed by silver staining as described above.

CAAT-Binding Protein Purification by DNA-Affinity Column Chromatography. The nuclear protein which interacts with the CAAT-region of the *MDR1* promoter in HL60/VCR nuclear extracts was purified using a DNA-sepharose affinity column as described (*26*). First, nuclear extracts (about 2−3 mg of protein) were precleared using the Microcon YM-50 (Millipore Corp., Bedford, MA) centrifugal filter device to remove low molecular weight (<50 kDa) proteins as described by the manufacturer. The cleared nuclear proteins were then subjected to a specific DNA-sepharose affinity column in the presence of the CAAT-deleted and GC-box oligomers (at 20-fold molar excess) and 4 μg of poly (dI·dC) to remove nonspecific DNA-binding proteins in 1 mL of DNA-binding buffer containing 0.04 M KCl. The DNA-

Table 1: Cell Survival Analysis

	IC_{50} [M] (fold resistance)[a]		
cell line	VCR	VBL	DOX
HL60	3.0×10^{-9}	5.1×10^{-9}	1.0×10^{-7}
HL60/Vinc	4.0×10^{-6} (1300)	3.1×10^{-6} (620)	8.0×10^{-7} (8)
HL60/VCR	7.0×10^{-6} (2300)	7.3×10^{-6} (1400)	2.0×10^{-6} (20)

[a] Fold resistance is the ratio of the IC_{50} values for HL60/Vinc and HL60/VCR cells to that of HL60 cells. The cells were treated with or without increasing concentration of drugs at 37 °C for 96 h in 96 well plates. The concentrations of drugs that reduced cell survival by 50% (IC_{50}) were calculated from cell survival plots obtained by MTT assay as described. The average of triplicate determinants in three independent experiments was used for the analysis.

sepharose affinity column was prepared using cyanogen bromide (CNBr)-activated sepharose 4B (Amersham Pharmacia Biotech, Piscataway, NJ) coupled with 200 μg of ds-CAAT oligomer in coupling buffer (0.1 M $NaHCO_3$, pH 8.3, and 0.5 M NaCl) at 25 °C for 1 h as described by manufacturer. After remaining active groups on the sepharose gel were blocked by adding 0.1 M Tris-HCl, pH 8.0 at 25 °C for 2 h, the uncoupled oligomers were washed three times sequentially with low and high pH buffer solutions (sodium acetate, pH 4.0, and Tris-HCl, pH 8.0, each containing 0.5 M NaCl), and the sepharose slurry was packed in a column with 0.8 mL of DNA-binding buffer. Following the binding of the nuclear proteins, the column was washed, and then the bound proteins were eluted with 500 μL of DNA-binding buffer in the presence of stepwise increasing KCl concentrations (0.2, 0.4, 0.6, 0.8, and 1.0 M). The KCl concentration in the eluted protein solutions was adjusted to 0.04 M for further analysis by SDS−PAGE followed by silver staining, EMSA, and DNase I protection assays. Silver staining was performed using the silver staining kit (Sigma, St. Louis, MO) as described by the manufacturer.

DNase I Protection Assay. DNase I protection assay was carried out using the core foot-printing kit (Promega) as described by manufacturer. In short, 2×10^4 cpm of the 241 bp *MDR1* promoter DNA probe, digested with *Sac*I at 37 °C for 2 h to obtain a singly end-labeled probe at the forward strand, was incubated with 0−80 μg nuclear extracts or 1−3 ng of the purified CAAT-binding protein in the presence of excess cold CAAT, GC-box, and 4 μg of poly (dI·dC) used as nonspecific competitor under the conditions described above. Then, the protein-bound DNA was treated with DNase I (1.5 units/mL) at 25 °C for 1 min in the presence of 0.5 mM Ca^{2+} and 1.0 mM Mg^{2+}. Following phenol/chloroform extractions, the digested probes were precipitated, resuspended in sequencing loading buffer, and separated on 12% sequencing gels and visualized by autoradiography.

RESULTS

Detection of Drug Resistance and P-gp Expression Characteristics in HL60, HL60/Vinc, and HL60/VCR Cells. The degree of drug resistance to vincristine (VCR), vinblastine (VBL), and doxorubicin (DOX) in HL60, HL60/Vinc, and HL60/VCR cells were analyzed by MTT cell survival assay, the IC_{50} value of each drug was determined from the cell survival plots as described, and the results are presented in Table 1. The data show that HL60/Vinc cells are resistant to VCR, VBL, and DOX (about 1300-, 620-, and 8-fold) compared to HL60 cells. The derivative of HL60/Vinc cells, HL60/VCR, isolated by stepwise selection in the presence of increasing concentration of VCR in our laboratory, displays high resistance to VCR (2300-fold), VBL (1400-fold), and DOX (20-fold) compared to HL60 cells (Table 1). One of the mechanisms involved in the high degree of drug resistance in HL60/Vinc and HL60/VCR cells can be attributed to their high P-gp expression levels, as determined by Western blot analysis using C219 monoclonal antibody that recognizes P-gp, as described (Figure 1). Figure 1 shows that while P-gp expression is detectable in HL60/Vinc (lane 2), it is highly expressed in HL60/VCR (lane 3), while P-gp levels were under detectable levels in HL60 cells (lane 1). Since HL60/VCR cells express higher amounts of P-gp compared to HL60/Vinc cells, the molecular mechanisms involved in the overexpression of P-gp were analyzed using HL60/VCR cells in the rest of this study.

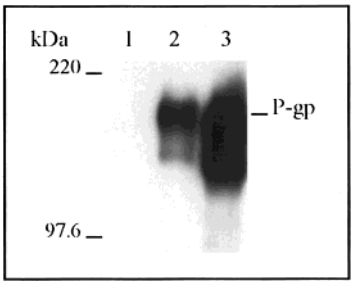

FIGURE 1: Determination of P-gp expression in HL60, HL60/Vinc, and HL60/VCR cells. The protein levels of P-gp (M_r 180 000) in HL60, HL60/Vinc, and HL60/VCR (lanes 1−3, respectively) cells were analyzed by Western blotting as described in Experimental Procedures. The total cellular proteins (80 μg/lane) were separated by 5−15% SDS−PAGE and P-gp levels were detected using the mouse monoclonal C219 antibody at a 1:1000 (w/v) dilution. Molecular weight markers are indicated on the left. The results shown are representative of two independent experiments.

Analysis of the MDR1 Gene Expression in HL60 and HL60/VCR Cells. To determine whether overexpression of P-gp is controlled at the mRNA level in HL60/VCR cells, RT-PCR was performed to detect *MDR1* mRNA levels as described. As seen in Figure 2A, a high level of *MDR1* mRNA was detected in HL60/VCR cells while it was under detectable levels in HL60 cells (lanes 3 and 2, respectively). The β-actin mRNA levels, used as internal controls, were similar in both of the cell lines (Figure 2A, lanes 5 and 4, respectively). These results show that the overexpression of P-gp is regulated at the mRNA level in HL60/VCR cells. To further investigate whether the high *MDR1* mRNA levels are due to increased levels of transcriptional initiation in HL60/VCR cells, nuclear run-on analysis was performed using the full-length 4.2 kb *MDR1* and 1.8 kb β-actin cDNA, used as an internal control, as described. Our results show that [α-^{32}P]UTP-labeled nuclear run-on transcripts of HL60/VCR detected high levels of *MDR1* cDNA (Figure 2B, panel 2, lower band), compared to that of HL60 cells (Figure 2B, panel 1), while β-actin cDNA was detected by labeled transcripts of both cell lines at similar levels (Figure 2B, upper band in panels 2 and 1, respectively), suggesting that *MDR1* mRNA expression is controlled by increased transcriptional initiation in HL60/VCR cells.

Identification of a Positive Regulatory Region in the MDR1 Promoter. To determine whether the transcriptional control of *MDR1* is mediated by increased promoter activity in

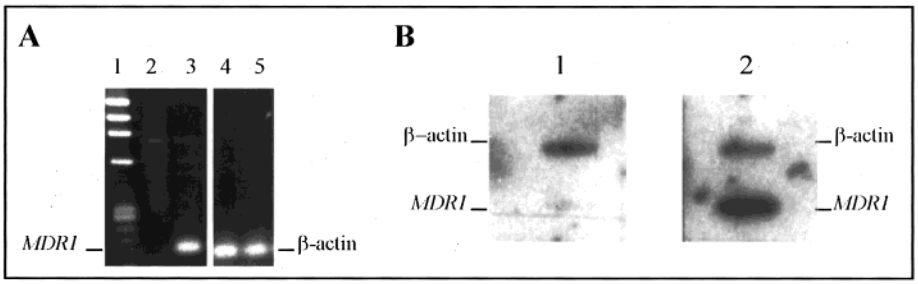

FIGURE 2: Analysis of *MDR1* transcription in HL60 and HL60/VCR cells. (A) The mRNA levels of *MDR1* in HL60 and HL60/VCR (lanes 2 and 3, respectively) were analyzed by RT-PCR. The β-actin mRNA levels in these cells (lanes 4 and 5, respectively) were used as internal controls. The RT-PCR products were run on 2% agarose gels and visualized by EtBr staining. Lane 1 contains *Hae*III-cut ϕX174 DNA fragments used as molecular weight markers. (B) The transcriptional initiation of the *MDR1* (lower band) and β-actin (upper band) genes in HL60 and HL60/VCR (panels 1 and 2, respectively) were analyzed by nuclear run-on assay as described in Experimental Procedures. Equal counts of [α-^{32}P]UTP-labeled nuclear run-on transcripts were hybridized with slot-blots containing full-length 4.2 kb *MDR1* and 1.8 kb β-actin cDNAs. The results shown above are representative of at least two independent experiments.

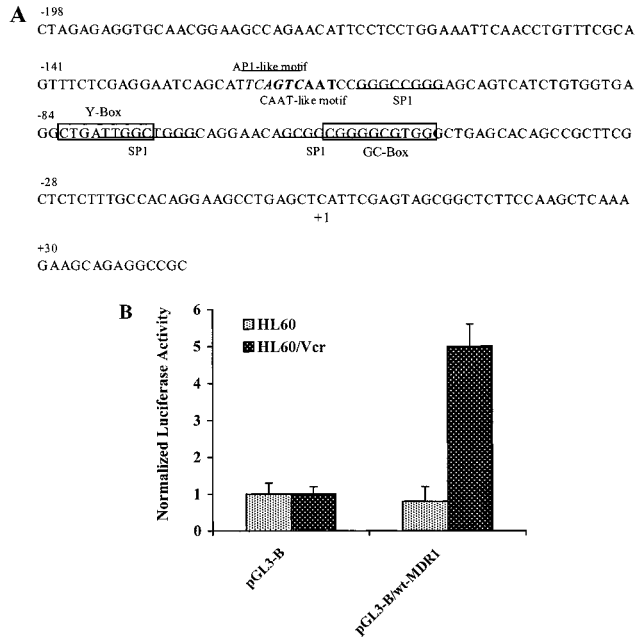

FIGURE 3: Analysis of *MDR1* promoter activity in HL60 and HL60/VCR cells. (A) The human *MDR1* proximal promoter DNA sequence, spanning residues between −198 to +43 with respect to the major transcriptional start site (+1), contains recognition sites such as SP1 (underlined), AP1 (overlined/italicized), Y-box, GC-box, and CAAT-like (in bold) motifs for various transcription factors. (B) The analysis of wt *MDR1* promoter activity was performed by luciferase assay as described in Experimental Procedures. The 241 bp *MDR1* promoter DNA fragment (−198 to +43) was cloned into the pGL3-basic (pGL3-B) vector upstream of the luciferase gene. After cotransfections, luciferase activity levels were measured in HL60 and HL60/VCR cells and normalized to their β-gal levels. Triplicate samples were used for each time point in two independent experiments. Error bars represent standard deviations.

HL60/VCR cells, the 241 bp *MDR1* promoter DNA fragment spanning the −198 to +43 region, containing AP1-like, CAAT-like, Y-box, and several SP1 recognition sites (Figure 3A), was cloned into the pGL3-basic vector upstream of the luciferase gene as described. *MDR1* promoter activity was measured as a function of luciferase activity, normalized to the β-gal levels reflecting equal transfection efficiency, following cotransfections of pGL3-basic plasmid constructs with the pSV-β-gal control plasmid into HL60 and HL60/VCR cells as described. As seen in Figure 3B, luciferase activity in HL60/VCR cells transfected with the plasmids containing the 241 bp *MDR1* promoter fragment were about 5.2-fold higher compared to that of HL60 cells, while in controls, where both HL60 and HL60/VCR cells transfected with the pGL3-basic plasmid alone, luciferase activity levels were similar. These results suggest that *MDR1* promoter activity is upregulated by positive regulatory transcription factor(s) in HL60/VCR cells, but not in HL60 cells. Therefore, in an attempt to identify the region(s) of the 241 bp *MDR1* promoter involved in upregulating its activity, the pGL3-promoter plasmids containing ds-oligomers with CAAT-like, CAAT-deleted, GC-box, and nonspecific fragments upstream of the SV-40 promoter and luciferase gene were constructed as described in Experimental Procedures. The effects of these fragments on the SV-40 promoter activity were measured as a function of luciferase activity normalized to the β-gal levels, after cotransfection of the HL60 and HL60/VCR cells with pGL3-promoter constructs and pSV/β-gal plasmids as described. The data show that the CAAT-like fragment resulted in a significant increase (about 7.8-fold) in SV-40 promoter activity in HL60/VCR transfectants compared to controls (Figure 4A). The CAAT-deleted, GC-box, and nonspecific fragments did not have a significant effect on the luciferase activity of the HL60/VCR transfectants expressing 1.7-, 1.8-, and 1.1-fold more luciferase activity compared to controls (Figure 4A). Similarly, these fragments did not have any significant effect on the activity of the SV-40 promoter in HL60 transfectants (Figure 4A). These results suggest that the CAAT-like region of the *MDR1* promoter is likely to interact with positive regulatory factor(s) in HL60/VCR cells but not in HL60 cells. To confirm that the CAAT-region is involved in upregulating *MDR1* promoter activity in HL60/VCR cells, the mutated 237 bp promoter DNA fragment, lacking the CAAT sequence, was created and cloned into the pGL3-basic vector upstream of the luciferase gene as described. The effects of the mutated *MDR1* promoter DNA fragment on its activity compared to the 241 bp wt promoter was assessed as a function of normalized luciferase activity levels by cotransfections of the HL60/VCR and HL60 cells as described above. Luciferase activity in HL60/VCR transfectants containing the CAAT-deleted 237 bp *MDR1* promoter sequence was reduced dramatically, almost to the levels of controls containing only plasmid itself, displaying only 1.6-fold higher activity, while the transfectants with the wt promoter sequence in HL60/VCR cells had about 6.4-fold more

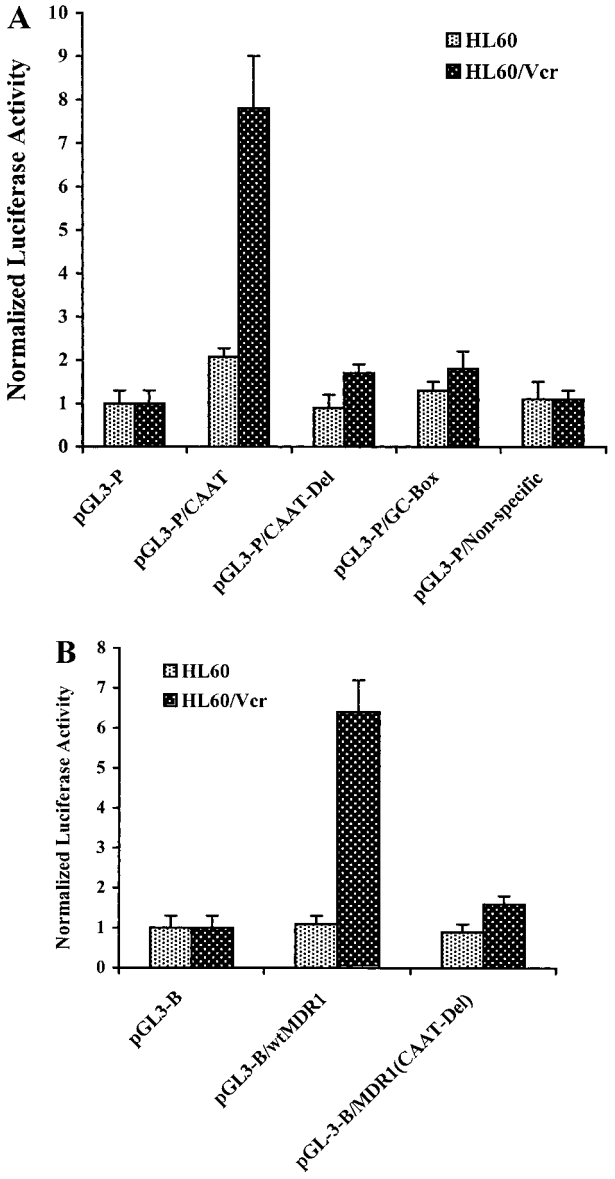

FIGURE 4: Determination of regions involved in the regulation of MDR1 promoter activity. (A) Analysis of the effects of oligomers containing CAAT-like, CAAT-deleted, GC-box, and nonspecific motifs on SV-40 promoter activity in HL60 and HL60/VCR cells. The ds-oligomers containing CAAT-like, CAAT-deleted, GC-box, and nonspecific motifs were cloned into the pGL3-promoter (pGL3-P) plasmid upstream of SV-40 promoter and luciferase gene as described in Experimental Procedures. The effects of these oligomers on the SV-40 promoter activity were measured as a function of luciferase activity following cotransfections of HL60 and HL60/VCR cells and luciferase activity levels were normalized to β-gal levels. (B) Analysis of wt and mutated (lacking CAAT) *MDR1* promoter activities in HL60 and HL60/VCR cells. The 241 bp wt and 237 bp mutated (CAAT-Del) *MDR1* promoter DNA fragments were cloned into the pGL3-basic vector upstream of the luciferase gene and luciferase activity levels in HL60 and HL60/VCR transfectants were measured and normalized to their β-gal levels as described above. The results shown above are representative of triplicate samples used in two independent experiments. Error bars represent standard deviations.

luciferase activity than controls (Figure 4B). The wt or mutated *MDR1* promoter fragments did not have any significant effect on luciferase activity in HL60 transfectants (Figure 4B). These results further suggest that the CAAT-region is involved in upregulating *MDR1* promoter activity by possibly interacting with positive regulatory nuclear factor(s) in HL60/VCR cells, but not in HL60 cells.

Detection of DNA-Binding Proteins Interacting with the CAAT-Region of the MDR1 Promoter in HL60/VCR Cells. To detect DNA-binding protein(s) interacting with the CAAT-region of the *MDR1* promoter, EMSAs were performed using a 5′-end labeled 241 bp ds-DNA probe, spanning the −198 to +43 region of the promoter, with nuclear extracts from HL60, HL60/Adr, HL60/Vinc, and HL60/VCR cells as described. Two major protein complexes (PC1 and PC2) that interact with the probe were detected in HL60/VCR cells (Figure 5A, lane 4). The PC1 of HL60/VCR cells seems to interact with the *MDR1* promoter probe specifically at the CAAT region, as revealed by its complete competition by excess cold probe and CAAT oligomer (Figure 5A, lanes 5 and 6, respectively), but not by excess (at 100-fold molar excess) CAAT-deleted, GC-box, nonspecific, AP1, SP1, NF-κB, C/EBP, or YY1 oligomers (Figure 5A, lanes 6−14, respectively). Interestingly, PC1 was not detectable in nuclear extracts of non-P-gp expressing HL60 and HL60/Adr cells (Figure 5A, lanes 2 and 3, respectively). The amount of PC1 in HL60/Vinc cells was about 3-fold less than that of HL60/VCR cells (Figure 5B, lanes 3 and 2, respectively), consistent with their P-gp expression levels. Moreover, PC2 did not compete with the cold probe or any other competitors in EMSAs, suggesting that it interacts with the probe nonspecifically. Similar results were obtained when the 5′-end labeled CAAT-oligomer was used as a probe in EMSAs with HL60/VCR nuclear extracts, showing that PC1 specifically interacts with the CAAT-region (Figure 6, lane 2). The excess cold CAAT oligomer completely inhibited PC1 (Figure 6, lane 3); however, its binding was not affected by CAAT-deleted, GC-box, or nonspecific oligomers at 100-fold molar excess (Figure 6, lanes 4−6, respectively). To assess the affinity of PC1 in HL60/VCR extracts for CAAT segment of the *MDR1* promoter, competition experiments were performed using increasing amounts of cold CAAT and CAAT-deleted oligomers at 0, 10, 25, 50, and 100-fold molar excess in EMSAs (Figure 7, lanes 1−5 and 6−10, respectively). As seen in Figure 7, CAAT oligomer at 25-fold molar excess significantly reduced the binding of PC1 (about 50%) to the CAAT-oligomer probe (lane 3). However, the CAAT-deleted oligomer did not affect the PC1−DNA interaction at 0−100 molar excess (Figure 7, lanes 6−10). Taken together, these results show that PC1, involved in upregulating MDR1 promoter activity, interacts with the *MDR1* promoter specifically and with a high affinity to the CAAT-segment in HL60/VCR cells.

Characterization of PC1 That Interacts with the CAAT Region of the MDR1 Promoter. To determine the molecular weight of PC1 which binds specifically the CAAT region of the *MDR1* promoter, UV cross-linking following EMSAs was performed and the cross-linked protein−DNA complexes were separated by 5−15% SDS−PAGE as described. Using HL60/VCR extracts and 5′-end labeled CAAT-oligomer probe, a single protein−DNA cross-linked complex with a total mass of about 150 kDa was detected (Figure 8, lane 1). The mass of the protein was estimated as 134 kDa by subtracting the mass of the probe, calculated as about 16 kDa (Figure 8, lane 1) from the total mass of the cross-linked complex. The specificity of the cross-linked protein was confirmed by its complete competition with excess amounts of cold CAAT, but not CAAT-deleted oligomer (Figure 8,

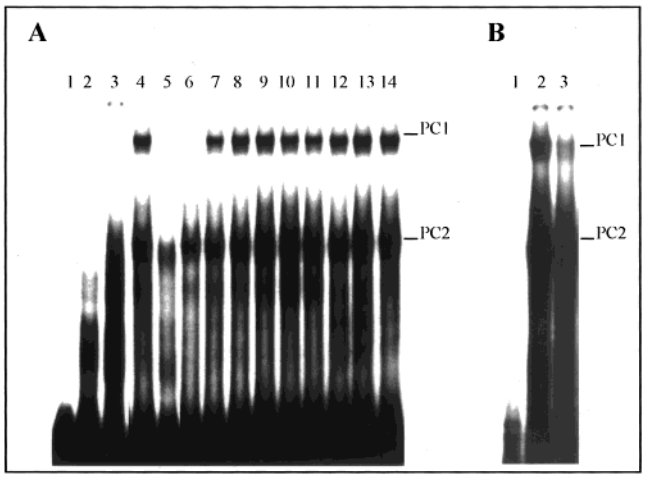

FIGURE 5: Detection of *MDR1* promoter binding proteins by EMSA in HL60 and HL60/VCR cells. (A) The 5′-end labeled 241 bp *MDR1* promoter DNA probe (−198 to +43) was incubated with nuclear extracts from HL60/VCR cells in the absence (lane 4) or presence of cold probe (lane 5), and oligomers containing CAAT-like, CAAT-deleted, GC-box, nonspecific, NF-κB, SP1, AP1, C/EBP, and YY1 (lanes 6−14, respectively) motifs at 100-fold molar excess in EMSAs. Panel A, lanes 2 and 3, contain nuclear extracts from non-P-gp expressing HL60 and HL60/Adr cells incubated with the probe. Panel B, lanes 2 and 3, contain nuclear extracts from HL60/VCR and HL60/Vinc, respectively, incubated with the probe. Lane 1 in Panels A and B contains unbound free probe. Protein−DNA complexes were separated on 5% native polyacrylamide gels and visualized by autoradiography. The results shown above are representative of at least three independent experiments.

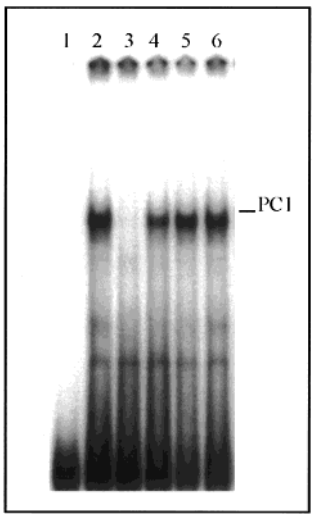

FIGURE 6: Detection of nuclear proteins interacting with the CAAT-region of the MDR1 promoter in HL60/VCR cells by EMSA. Nuclear extracts from HL60/VCR cells were incubated with the 5′-end labeled ds-CAAT-like oligomer probe in the absence (lane 2) or presence of cold probe (lane 3) and oligomers containing CAAT-deleted, GC-box, and nonspecific (lanes 4, 5, and 6, respectively) motifs in EMSAs. Lane 1 contains free probe. Protein−DNA complexes were run on 5% native polyacrylamide gels and visualized by autoradiography. Results shown are representative of at least three independent experiments.

lanes 2 and 3, respectively). Moreover, to confirm the estimated molecular mass of the PC1 in UV cross-linking experiments, Southwestern blot analysis was performed. A 128 kDa protein, interacting with the 5′-end labeled CAAT oligomer probe in HL60/VCR extracts, was identified in Southwestern analysis (Figure 9, lane 1), which was com-

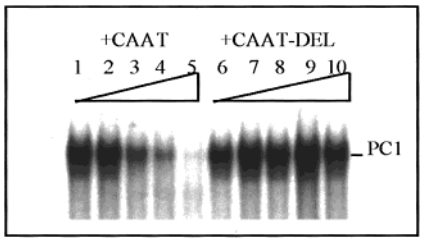

FIGURE 7: Determination of the affinity of the *MDR1* promoter-binding protein complex (PC1) to the CAAT-motif. The affinity of the PC1 complex for the CAAT-segment of the *MDR1* promoter is determined by incubating HL60/VCR nuclear extracts with the 5′-end labeled CAAT oligomer probe in the absence or presence of increasing concentrations of cold oligomers at 0, 10, 25, 50, and 100-fold molar excess containing CAAT (lanes 1−5, respectively) and CAAT-deleted (lanes 6−10, respectively) motifs in EMSAs as described previously. The results shown are representative of two independent experiments.

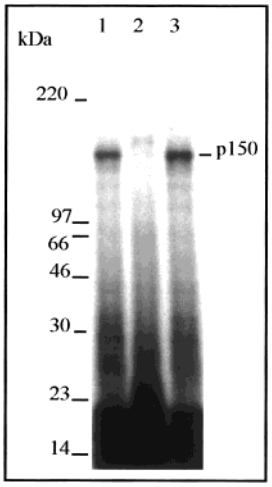

FIGURE 8: UV cross-linking analysis of nuclear proteins interacting with the CAAT-segment of the *MDR1* promoter. The 5′-end-labeled CAAT-like oligomer probe was incubated with the HL60/VCR nuclear extracts in the absence (lane 1) or presence of cold probe (lane 2) and CAAT-deleted oligomer (lane 3) under EMSA conditions described previously. Protein−DNA complexes were then exposed to UV light (302 nm) for 30 min on ice, determined as the optimum time point for cross-linking as described in Experimental Procedures, separated by 5−15% SDS−PAGE and visualized by autoradiography. The molecular weight markers are indicated on the left. The results shown above are representative of three independent experiments.

pletely competed in the presence of excess cold probe (Figure 9, lane 2). No signal was detected using HL60 extracts in Southwestern blot analysis (Figure 9, lanes 3 and 4, respectively). These results together show that the molecular mass of the protein interacting with the CAAT-region is most likely around 130 kDa. In addition, to determine whether PC1 contains other subunit(s) with low or no DNA-binding ability, EMSAs with HL60/VCR nuclear extracts and CAAT oligomer probe were performed (Figure 10A, lanes 1−3). The PC1 bands were then excised from polyacrylamide gels. Following electroelution, PC1 was subjected to 5−15% SDS−PAGE and analyzed by silver staining (Figure 10B). Interestingly, silver staining of the electroeluted protein revealed that it contains two polypeptides with molecular masses of about 130 and 162 kDa (Figure 10B). These results further suggest that the p130 is the DNA-binding factor of the complex, consistent with its molecular mass obtained from UV cross-linking and Southwestern blot analysis

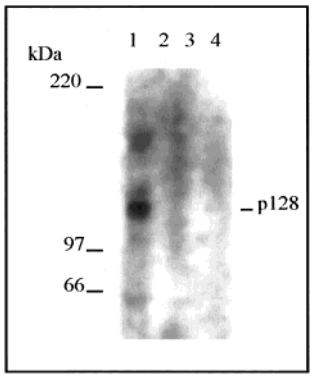

FIGURE 9: Southwestern blot analysis of nuclear proteins interacting with the CAAT-segment of the *MDR1* promoter. Nuclear extracts from HL60/VCR (lanes 1−2) and HL60 (lanes 3−4) cells were separated by 5−15% SDS PAGE containing 6.5 M urea and blotted onto an Immobilon membrane as described. The membranes were then incubated with the 5′-end labeled CAAT-like oligomer probe in the absence (lanes 1 and 3) or presence of cold probe (lanes 2 and 4). The DNA−protein complexes were visualized by autoradiography. The molecular weight markers are indicated on the left. The results shown are representative of two independent experiments.

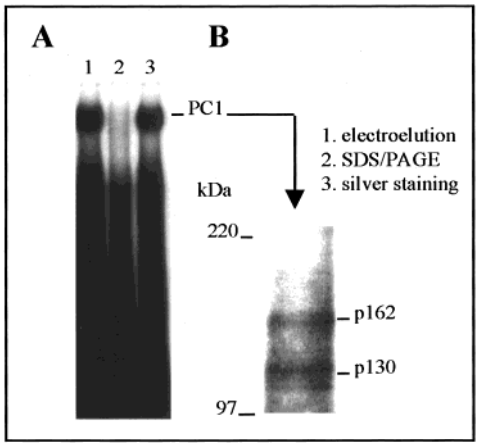

FIGURE 10: Analysis of electroeluted PC1 complex by silver staining following EMSA. (A) Nuclear extracts from HL60/VCR cells were incubated with the 5′-end labeled CAAT-like oligomer probe (lane 1) in the presence of cold probe and GC-box (lanes 2 and 3, respectively) oligomers as described in EMSA. (B) The PC1 complex interacting with the CAAT-segment of the *MDR1* promoter was then excised from polyacrylamide gels, electroeluted and separated by 5−15% SDS−PAGE. The proteins were visualized by silver staining as described in Experimental Procedures. Molecular weight markers are indicated on the left. The results shown are representative of three independent experiments.

(Figures 8 and 9, respectively). However, the p162 was not detectable in cross-linking or Southwestern blot analyses, suggesting that it has a low binding affinity to the CAAT oligomer probe or that it might not have DNA-binding ability. As a control, the nonspecific PC2 was excised, electroeluted, and analyzed by silver staining as described above. Neither p130 nor p162 were detected in eluted PC2 (data not shown), confirming that they are specific for PC1, and they do not represent any contaminating peptides during electroelution. However, the presence of minor bands in the silver-stained gel containing electroeluted PC1 (Figure 10B) suggests that some other polypeptides might interact with MDR1 promoter with lower affinity. They might also represent some contaminating peptides coeluted with PC1,

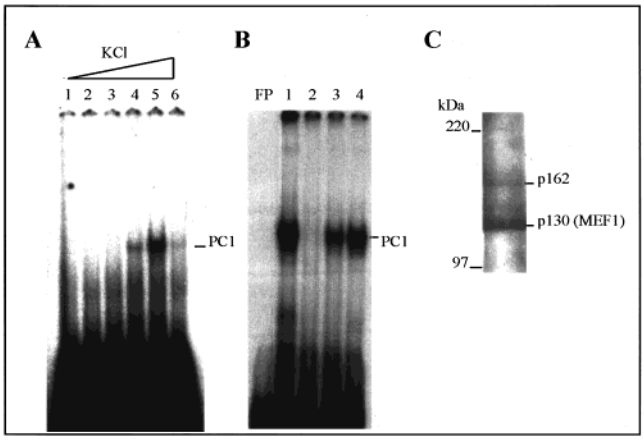

FIGURE 11: Purification of the PC1 complex using DNA-sepharose affinity column. (A) PC1 complex interacting with the CAAT-segment of the *MDR1* promoter was purified using a specific DNA-sepharose affinity column conjugated with the cold CAAT-like oligomer as described in Experimental Procedures. The proteins bound to the CAAT-column were eluted sequentially with 0, 0.2, 0.4, 0.6, 0.8, and 1.0 M KCl, (lanes 1−6, respectively) and eluates were incubated with the 5′-end-labeled CAAT-like oligomer probe in EMSAs as described. Protein−DNA complexes were separated in 5% native polyacrylamide gels and visualized by autoradiography. (B) Nuclear extracts from HL60/VCR cells were incubated with the CAAT-oligomer probe in the absence (lane 1) or presence of cold probe (lane 2) and oligomers containing CAAT-deleted and GC-box (lanes 3 and 4, respectively) in EMSAs. Lane FP contains unbound free probe. (C) The PC1 complex purified using DNA-sepharose affinity column and eluted in the presence of 0.8 M KCl was separated by 5−15% SDS−PAGE and visualized by silver staining. Molecular weight markers are indicated on the left. The results shown are representative of two independent experiments.

since similar minor bands were also observed in the electroeluted PC2 controls (data not shown).

Purification and Characterization of the PC1 by Specific DNA-Affinity Chromatography. The PC1 that binds specifically the CAAT-region of the *MDR1* promoter was purified from HL60/VCR extracts using a DNA-sepharose affinity column conjugated with the CAAT oligomer as described in Experimental Procedures. The protein fractions that bind the column were eluted with stepwise increasing concentrations of KCl (Figure 11A, lanes 1−6), and their functional integrity and specificity were analyzed by EMSAs with labeled CAAT oligomer probe. As Figure 11A shows, fractions eluted with 0.6, 0.8, and 1.0 M KCl (lanes 4, 5 and 6, respectively), but not with 0.1, 0.2, and 0.4 M KCl (lanes 1−3, respectively), interacted with the CAAT probe, as revealed by a strongly shifted PC1 band identical to that obtained with total nuclear extracts in the absence or presence of excess cold CAAT, CAAT-deleted, and GC-box oligomers (Figure 11B, lanes 1−4, respectively). To determine the molecular mass of the fraction eluted with 0.8 M KCl, silver staining following SDS−PAGE was performed (Figure 11C). Consistent with our previous results obtained using eletroeluted PC1 from polyacrylamide gels following EMSAs, p130 and p162 were detected in the 0.8 M KCl fraction (Figure 11C). These results strongly suggest that PC1 consists of two components and that p130, which we refer to as *MDR1*-promoter *e*nhancing *f*actor 1 (MEF1), has a strong DNA-binding ability, with a high specificity to the CAAT region of the *MDR1* promoter. As seen in Figure 11C, there were no minor bands in the silver-stained gel, indicating that

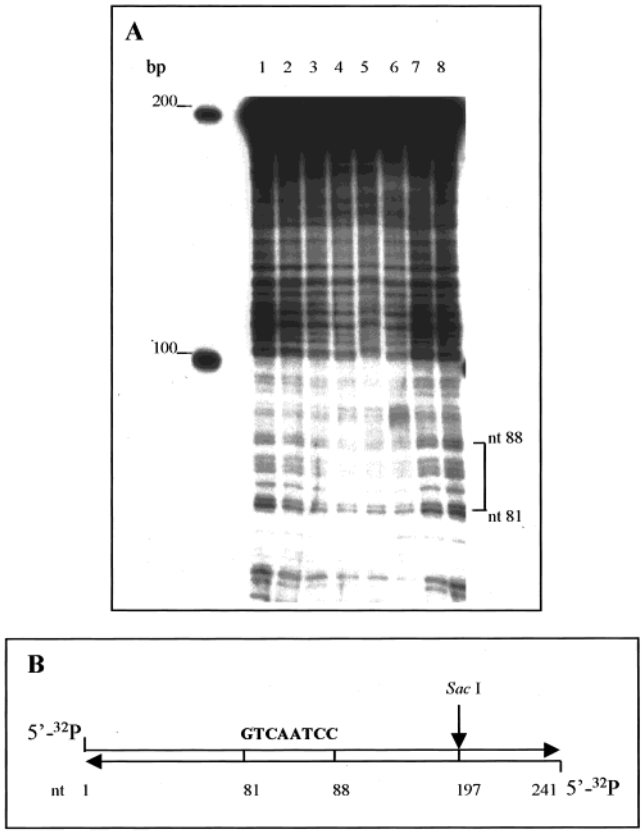

FIGURE 12: DNase I protection assay for the analysis of the wt *MDR1* promoter DNA. (A) The 5′ singly end-labeled *MDR1* promoter probe (197 bp), generated by *Sac*I digestion, incubated with DNase I in the absence (lanes 1 and 8) or presence of 40, 60, and 80 μg HL60/VCR nuclear extracts (lanes 2−4, respectively) or DNA affinity column purified MEF1 eluted with 0.8 M KCl (lane 5). Protection of the probe was observed in a region spanning nucleotides −81 to −88. The presence of excess cold CAAT (lane 7), but not GC-box (lane 6), oligomer inhibited the protection of this region in the presence of 80 μg nuclear extracts. One hundred base pair [^{32}P]-labeled molecular weight markers are indicated on the left. The protected regions are indicated on the right. The results shown are representative of three independent experiments. (B) The 5′ singly end-labeled *MDR1* promoter DNA probe (197 bp), generated by digestion of the 241 bp *MDR1* promoter DNA with *Sac*I, contains the GTCAATCC sequence between nucleotides −81 to −88. The figure is not drawn to scale.

the purification of PC1 by DNA affinity chromatography is much more specific than purification by electroelution (Figure 10B).

Identification of MEF1-Binding Sites on the MDR1 Promoter by DNase I Protection Assay. Protein-binding site using 0, 40, 60, and 80 μg of HL60/VCR crude extracts and the *MDR1* promoter probe labeled at the 5′ end of the coding (forward) strand, generated by Sac I digestion, was determined by DNase I protection assay (Figure 12A, lanes 1−4, respectively). As shown in Figure 12A, lanes 1−4, the most strongly protected region covers nucleotides −81 to −88. The protection of this region was inhibited by the presence of excess CAAT oligomer, but not GC-box oligomer (Figure 12A, lanes 7 and 6, respectively). As Figure 12A shows, the use of the affinity chromatography purified fraction eluted with 0.8 M KCl with the forward *MDR1* probe resulted in protection of the nucleotides −81 to −88 (lane 5), compared to the DNase I digested probe in the absence of protein (Figure 12A, lanes 1 and 8). Moreover, as shown in Figure 12B, the 5′ singly end-labeled MDR1 promoter probe (197 bp), generated by *Sac*I digestion, contains the 5′-GTCAATCC-3′ sequence between nucleotides −81 to −88.

DISCUSSION

Multidrug resistant HL60/VCR human AML cells display high resistance to VCR, VBL, and DOX, compared to sensitive HL60 cells. The multidrug resistant phenotype can be attributed to overexpression of P-gp in these cells. The molecular mechanisms underlying the overexpression of P-gp in HL60/VCR cells are not well-known. This study shows that P-gp expression is regulated at the transcriptional level, specifically by increased transcriptional initiation of the *MDR1* gene in this cell line. The data presented in this study also provide evidence that the *MDR1* promoter is activated by a nuclear complex that specifically interacts with the CAAT-region. Our results indicate that this nuclear factor consists of two polypeptides with molecular masses of about 130 and 162 kDa, as determined by DNA-sepharose affinity column and electroelution following EMSA. Moreover, Southwestern and cross-linking analysis showed that only p130, referred to as MEF1, seems to bind the CAAT-region of the *MDR1* promoter with high affinity and specificity. The function of p162 is not known and remains to be determined. However, it might act as an ancillary protein to MEF1, as observed in Ets family members in which GAPBα binding to DNA is greatly enhanced by GAPBβ (*27*). Similarly, two component factors, consisting of DNA-binding protein p37 and its partner p49 that does not bind DNA but is necessary for strong binding of p37, were reported to be involved in silencing the adenine nucleotide translocator isoform 2 (ANT2) in HeLa cells (*28*). Moreover, DNase I protection assay implies that MEF1 interacts with the 5′-GTCAATCC-3′ element of the *MDR1* promoter. In addition, deletion of the CAAT motif in EMSAs almost completely abolished the binding of MEF1 to the *MDR1* promoter DNA fragment, suggesting that CAAT is the core binding element of MEF1. Furthermore, this was evident in transient trasfections of HL60/VCR cells with the mutated *MDR1* promoter, lacking CAAT, DNA fragment/luciferase plasmid constructs in which no change in luciferase activity was detected, whereas transfectants containing the wt *MDR1* promoter or CAAT-like oligomer/luciferase plasmids expressed about 5−7-fold more luciferase activity compared to controls. Taken together, these results suggest that MEF1 might be a CAAT-binding protein, although its recognition element is slightly different than the typical CCAAT-box motif. No known protein was obtained from a search of the GenBank for nuclear factors recognizing GTCAATCC hexanucleotide element with a molecular mass of about 130 kDa, indicating that MEF1 might be a novel transcription factor involved in activating the *MDR1* promoter in HL60/VCR cells. This, however, needs further investigation.

In addition, MEF1 was not detected in EMSAs using nuclear extracts from sensitive HL60 and drug resistant non-P-gp expressing HL60/Adr cells, consistent with its involvement in upregulating *MDR1* promoter activity. Similarly, MEF1 was not detectable in P-gp overexpressing MCF-7/Adr human breast cancer cells (data not shown). Thus, these results suggest that the control of *MDR1* promoter activity could be cell line or tissue specific, which is consistent with previous studies in which many positive or negative regula-

tory proteins were reported to play a role in its control in different cell lines (*14*, *19*). Recently, it was also reported that there is an inverse correlation between methylation and *MDR1* expression in clinical AML samples (*29*), suggesting that hypomethylation of CpG sites on the *MDR1* promoter might be required for the expression of *MDR1* mRNA (*30*). It is not known, however, whether there is a relation between the methylation status of the *MDR1* promoter and MEF1 binding in HL60/VCR nuclear extracts.

There is evidence indicating that mutated p53 and P-gp expression is often coexpressed and associated with a poor prognosis in human breast cancer cells (*31*). It has also been suggested that wild-type p53 interacts with various regions of the MDR1 promoter and is involved in the negative regulation of its activity in the Saos-2 and BHK cell lines (*32*). However, the control of *MDR1* transcription in HL60 or its drug-resistant derivative HL60/VCR cells is p53-independent since these cells do not express p53 (*33*, *34*). Moreover, it should be noted that HL60/VCR cells are very resistant to VCR and VBL (which target tubulin), displaying more than 1000-fold more resistance compared to HL60 cells. In contrast, these cells display lower resistance to DOX (which targets DNA), about 20-fold, compared to HL60 cells, suggesting that non-P-gp related mechanisms may contribute to the high levels of resistance to VCR and VBL in HL60/VCR cells. However, we also showed that MEF1 is overexpressed in HL60/Vinc cells expressing lower resistance to *Vinca* alkaloids. Our data demonstrate the role of MEF1 in regulating MDR1 expression, but the molecular mechanisms of how it increases transcription of this gene remains to be found.

ACKNOWLEDGMENT

We would like to thank Dr. Mary D. McCauley for her editorial assistance. Direct sequencing of cDNA fragments isolated from agarose gels was performed by the DNA Sequencing Facility in the Department of Biochemistry at the Medical University of South Carolina.

REFERENCES

1. Safa, A. R. (1998) *Methods Enzymol. 292*, 289−307.
2. Fairchild, C. R., Moscow, J. A., O'Brien, E. E., and Cowan, K. H. (1990) *Mol. Pharmacol. 37*, 801−9.
3. Guild, B. C., Mulligan, R. C., Gros, P., and Housman, D. E. (1988) *Proc Natl Acad Sci* USA *85*, 1595−9.
4. Fojo, A. T., Ueda, K., Slamon, D. J., Poplack, D. G., Gottesman, M. M., and Pastan, I. (1987) *Proc. Natl. Acad. Sci. U.S.A. 84*, 265−9.
5. Bell, D. R., Gerlach, J. H., Kartner, N., Buick, R. N., and Ling, V. (1985) *J. Clin. Oncol. 3*, 311−5.
6. Bourhis, J., Goldstein, L. J., Riou, G., Pastan, I., Gottesman, M. M., and Benard, J. (1989) *Cancer Res. 49*, 5062−5.
7. Nooter, K, and Sonneveld, P. (1994) *Leuk. Res. 18*, 233−43.
8. Del Poeta, G., Venditti, A., Stasi, R., Aronica, G., Cox, M. C., Buccisano, F., Tamburini, A., Bruno, A., Maurillo, L., Battaglia, A., Suppo, G., Epiceno, A. M., Del Moro, B., Masi, M., Amadori, S., and Papa, G. (1999) *Leuk. Res. 23*, 451−65.
9. Zhou, D. C., Zittoun, R., and Marie, J. P. (1995) *Leukemia 9*, 1661−6.
10. Zochbauer, S., Gsur, A., Brunner, R., Kyrle, P. A., Lechner, K., and Pirker, R. (1994) *Leukemia 8*, 974−7.
11. Leith, C. P., Kopecky, K. J., Godwin, J., McConnell, T., Slovak, M. L., Chen, I. M., Head, D. R., Appelbaum, F. R., and Willman, C. L. (1997) *Blood 89*, 3323−9.
12. Musto, P., Melillo, L., Lombardi, G., Matera, R., di Giorgio, G., and Carotenuto, M. (1991) *Br. J. Haematol. 77*, 50−3
13. Madden, M. J., Morrow, C. S., Nakagawa, M., Goldsmith, M. E., Fairchild, C. R., and Cowan, K. H. (1993) *J. Biol. Chem. 268*, 8290−7.
14. Sundseth, R., MacDonald, G., Ting, J., and King, A. C. (1997) *Mol. Pharmacol. 51*, 963−71.
15. Ohga, T., Uchiumi, T., Makino, Y., Koike, K., Wada, M., Kuwano, M., and Kohno, K. (1998) *J. Biol. Chem. 273*, 5997−6000.
16. Rohlff, C., and Glazer, R. I. (1998) *Int. J. Oncol. 12*, 383−6.
17. Jin, S., and Scotto, K. W. (1998) *Mol. Cell. Biol. 18*, 4377−84.
18. Ogura, M., Takatori, T., Sugimoto, Y., and Tsuruo, T. (1991) *Jpn. J. Cancer Res. 82*, 1151−9.
19. Ogretmen, B., and Safa, A. R. (1999) *Biochemistry 38*, 2189−99.
20. Ogretmen, B., Bahadori, H., McCauley, M., Boylan, A., Green, M., and Safa, A. R. (1998) *Cancer Chemother. Pharmacol. 42*, 441−6.
21. Ogretmen, B., and Safa, A. R. (1996) *Int. J. Cancer 67*, 608−14.
22. Ogretmen, B., and Safa, A. R. (1995) *Biotechniques 19*, 374−6.
23. Ogretmen, B., Ratajczak, H., Kats, A., Stark, B. C., and Gendel, S. M. (1993) *Biotechniques 14*, 932−5.
24. Ogretmen, B., McCauley, M. D., and Safa, A. R. (1998) *Biochemistry 37*, 11679−91.
25. Czyzyk-Krzeska, M. F., and Bendixen, A. C. (1999) *Blood 93*, 2111−20.
26. Kadonaga, J. T., and Tjian, R. (1986) *Proc. Natl. Acad. Sci. U.S.A. 83*, 5889−93.
27. Thompson, C. C., Brown, T. A., and McKnight, S. L. (1991) *Science 253*, 762−8.
28. Barath, P., Albert-Fournier, B., Luciakova, K., and Nelson, B. D. (1999) *J. Biol. Chem. 274*, 3378−84.
29. Desiderato, L., Davey, M. W., and Piper, A. A. (1997) *Somat. Cell Mol. Genet. 23*, 391−400.
30. Nakayama, M., Wada, M., Harada, T., Nagayama, J., Kusaba, H., Ohshima, K., Kozuru, M., Komatsu, H., Ueda, R., and Kuwano, M. (1998) *Blood 92*, 4296−307.
31. Linn, S. C., Honkoop, A. H., Hoekman, K., van der Valk, P., Pinedo, H. M., and Giaccone, G. (1996) *Br. J. Cancer 74*, 63−8.
32. Strauss, B. E., Shivakumar, C., Deb, S. P., Deb, S., and Haas, M. (1995) *Biochem. Biophys. Res. Commun. 217*, 825−31.
33. Shimizu, T., and Pommier, Y. (1996) *Exp. Cell Res. 226*, 292−301.
34. Takagi, M., Shigeta, T., Asada, M., Iwata, S., Nakazawa, S., Kanke, Y., Ishimoto, K., and Mizutani, S. (1999) *Leukemia 13*, 70−7.

BI991943F